**7B.5** **THE HURRICANE-CUSTOMIZED EXTENSION OF THE VAD (HEVAD) METHOD: HURRICANE WIND ESTIMATION IN THE LOWER TROPOSPHERE**

Paul R. Harasti* and Roland List
University of Toronto, Toronto, Ontario, Canada

## 1. INTRODUCTION

This paper presents a new single-Doppler radar analysis method that estimates the *earth-relative* wind field of hurricanes in the Lower Troposphere (LT - altitude ≤ 3 km). Other methods currently in use include the GBVTD (Lee et al., 1999) and TREC (Tuttle and Gall, 1999) methods. The GBVTD method estimates the *storm-relative* wind field in hurricanes and thus requires extraneous information about the mean flow across the hurricane in order to obtain earth-relative winds for hurricane forecasting purposes. The TREC method also estimates the *earth-relative* wind field. However, as with all single-Doppler analysis methods, violations of the underlying assumptions made about the wind field bias the results either in certain regions or certain situations. The GBVTD and TREC methods are most accurate in the regions near and far from the hurricane's core, respectively. It is hoped that the current approach will bridge the gap of information in the intermediate region, and perhaps provide mean flow estimates to the GBVTD method so that a complete picture of the earth-relative wind field can be delivered to forecasters.

## 2. THE HURRICANE-CUSTOMIZED EXTENSION OF THE VAD (HEVAD) METHOD

The tangential wind component of most mature hurricanes is strongly axisymmetric in the lower troposphere with an asymmetric and radial wind component of less than 10% (Willoughby, 1995). Thus, it is appropriate to develop Doppler radar analysis methods for axisymmetric hurricane circulations.

Donaldson (1991) showed how the VAD method (Browning and Wexler, 1968) could be used to estimate the shearing deformation and the tangential and radial wind components of axisymmetric hurricanes. Harasti and List (1995) extended this methodology to include the stretching deformation, divergence and inflow angle of the winds. Both methods estimate the stated quantities along a vertical axis passing through the radar; only the method of Harasti and List extrapolates the winds beyond this axis in the horizontal direction. The HEVAD method, now presented, greatly improves upon the accuracy of this extrapolation and also provides estimates of the mean flow across the hurricane in the LT.

The HEVAD method requires a single volume scan of Doppler velocity data that includes several PPIs in the range $\sim 0.5^\circ \le \theta \le \sim 10^\circ$. The method assumes that the tangential ($V_t$) and radial ($V_r$) wind components of the hurricane can be approximated by a modified-Rankine vortex:

$$V_i(\zeta,z) = V_i(R,z)[R/\zeta]^{X_i}, \quad (1)$$

where $i = t$ and $i = r$ for the tangential and radial winds, respectively. $V_i$ is the magnitude of the particular wind component at the radial distance $\zeta$ from the circulation center and at the altitude **z** within the LT. The analysis is restricted to the region $\zeta \ge \zeta_m$, where $\zeta_m$ is the radius of maximum wind. The radar is located at $\zeta = R$.

The PCA method (Harasti and List, 2001) is first used to estimate **R,** $\zeta_m$ and the radar-azimuth angle of the circulation center, $\phi_C$. The spherical coordinate system of the radar is then rotated $\phi_C$ degrees clockwise from true north so that its **x** and **y** axes are parallel to $V_t$ and $V_r$, respectively, at the radar site. Fig. 1 shows the HEVAD coordinate system as seen through the plane of any VAD circle at altitude **z**. **u** and **v** are the Cartesian components of the horizontal wind whose Doppler components are measured at the range **r** from the radar located at **O**. $\beta$ is the azimuth angle measured from the circulation center at **C**, and $\theta$ is the elevation angle of the PPI.

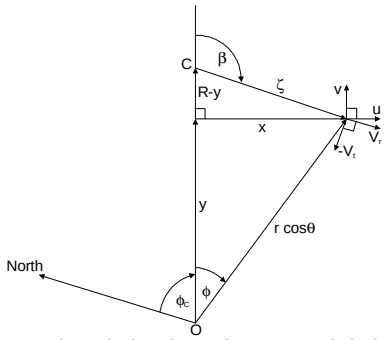


Fig. 1. Geometry through the plane of any VAD circle in the HEVAD coordinate system. See text for details.

In the HEVAD coordinate system, the wind components are related according to

$$u(\zeta,z) = V_r(\zeta,z)\sin\beta - V_t(\zeta,z)\cos\beta \quad (2)$$

$$v(\zeta,z) = V_r(\zeta,z)\cos\beta + V_t(\zeta,z)\sin\beta. \quad (3)$$

The HEVAD method customizes the results of Caya and Zawadski (1992) for the particular case of a non-linear wind field defined by (1). The customization is accomplished by evaluating the horizontal derivatives of a Taylor series expansion of **u** and **v** about **O**. In order to accomplish this, it is necessary to use (2) and (3) along with the trigonometric relations between $(\zeta,\beta)$ and $(x,y)$ inferred from Fig. 1, then evaluate the series coefficients at $(x,y) = (0,0)$. The results are as follows:

* *Corresponding Author Address:* Dr. Paul R. Harasti, National Center for Atmospheric Research, P.O. Box 3000, Boulder, CO 80307-3000; e-mail: harasti@ucar.edu.

$$a_0 = V_r(R,z)\sum_{i=0}^{\infty}\Gamma_{0i}^{a}\left[\frac{r}{R}\right]^{2i+1}[\cos\theta]^{2i+2} + W_{a0}\sin\theta$$

$$a_n = V_r(R,z)\sum_{i=0}^{\infty}\Gamma_{ni}^{a}\left[\frac{r}{R}\right]^{2i+n-1}[\cos\theta]^{2i+n} + W_{an}\sin\theta, \quad n \geq 1$$

$$b_n = V_t(R,z)\sum_{i=0}^{\infty}\Gamma_{ni}^{b}\left[\frac{r}{R}\right]^{2i+n-1}[\cos\theta]^{2i+n} + W_{bn}\sin\theta, \quad n \geq 1$$

where the Fourier coefficients $a_0$, $a_n$ and $b_n$ are determined via a least-squares solution to

$$V_D(\phi) = a_0 + \sum_{n=1}^{m}[a_n\cos n\phi + b_n\sin n\phi] \qquad (4)$$

for the Doppler velocity data around each VAD circle, $V_D(\phi)$. $\Gamma_{ni}^{a}$ and $\Gamma_{ni}^{b}$ are polynomial functions of $X_r$ and $X_t$, respectively. For example, $\Gamma_{00}^{a} = -(X_r - 1)/2$, $\Gamma_{10}^{a} = -\Gamma_{10}^{b} = -1$, $\Gamma_{20}^{a} = -(X_r + 1)/2$, $\Gamma_{20}^{b} = (X_t + 1)/2$ and $\Gamma_{30}^{b} = (X_t + 1)(X_t + 3)/8$ are the leading terms used in the HEVAD method. Thus, each Fourier coefficient is represented by an infinite power series expansion in either even or odd powers of $r/R$, with each successive term in the series smaller than the previous terms. In order for (4) to fit the wind field exactly, it also follows that, in principle, $m = \infty$; however, only the terms up to $m = 3$ are required by the HEVAD method. The magnitude of the leading terms of each of these coefficients dominates the sum of the remaining terms, which are ignored. Upper bounds on $r/R$ are chosen to minimize the biases due to these ignored terms (see below). The "**W**" terms contain the Taylor series coefficients for the vertical motion of the hydrometeors. These terms are also ignored but their resulting biases are minimized by correcting $V_D(\phi)$ for the terminal fall speed of the hydrometeors, using standard reflectivity-fall speed relationships, and by setting limits on $\theta$.

In order to estimate the earth-relative winds, it is necessary to superimpose a uniform wind on (1) to represent the mean flow across the hurricane that is a function of **z**. The components of the mean flow, $u_m$ and $v_m$, are simply added to $b_1$ and $a_1$, respectively. The leading terms of (4) up to $m = 3$, yield:

$$V_t(R,z) \approx 2Rb_2/([1 + X_t]r\cos^2\theta) \qquad (5)$$

$$V_r(R,z) \approx -2Ra_2/([1 + X_r]r\cos^2\theta) \qquad (6)$$

$$u_m(z) \approx -V_t(R,z) + b_1/\cos\theta \qquad (7)$$

$$v_m(z) \approx V_r(R,z) + a_1/\cos\theta \qquad (8)$$

$$X_t \approx -3 + 4Rb_3/(b_2 r\cos\theta) \qquad (9)$$

$$X_r \approx (a_2 + a_0)/(a_2 - a_0) \qquad (10)$$

Individual results from (9) and (10) tend to have large variances from their means, comparable in magnitude to their means. Therefore, the results of (9) and (10) are averaged throughout the range of **z** spanned by their restricted VAD circles (see below); these averages are assumed to be representative of the entire LT. (9) is a very robust estimate of $X_t$ in the LT since $b_2$ and $b_3$ are dominated by the tangential wind that is predominantly axisymmetric. In comparison, (10) tends to be more susceptible to the relatively large $W_{a0}$ term in $a_0$. However, if the sign of $V_r \approx R[a_0 - a_2]/r$ (follows from substituting (10) into (6)) is negative, thus indicating inflow, the approximation $X_r \approx X_t$ may be utilized in (6) instead. Such an approximation implies that the inflow angle is a constant in the LT. This approximation has been confirmed by numerous case studies of hurricanes.

Lower bounds on $r/R$ are also necessary to obtain a minimum precision in the estimates because the magnitudes of the coefficients used in (5), (6), (9) and (10) are proportional to powers of $r/R$. These lower bounds, as well as the above-mentioned upper bounds, were determined using a model for the Doppler velocity that included (1), Gaussian noise and estimates of the "**W**" terms. With **R** fixed in each simulation, $r/R$ was incremented from its lowest value until running averages of (5)-(10) from 10 consecutive VAD circles returned stable estimates of the parameters; these limits set the lower bounds. $r/R$ was then incremented beyond its lower bound until the bias in the estimated parameters just exceeded 5%; these limits set the upper bounds. A similar procedure was used to set the upper bounds on $\theta$. The conclusions of these simulations were that (5)-(8) require $0.1 \leq r/R < 0.6$ and $\theta \leq 10^\circ$, (9) requires $0.3 \leq r/R < 0.6$ and $\theta \leq 2.5^\circ$, and (10) requires $0.15 \leq r/R < 0.45$ and $\theta \leq 1.5^\circ$.

The Fourier coefficients are only independent when the data are equally spaced around the VAD circles. Therefore, the presence of missing or unequally spaced data requires $m > 3$ in the fit (4) in order to obtain unbiased estimates of the coefficients used in (5)-(10). The results of simulations also showed that better than ~5% accuracy of (5)-(10) is achieved provided that **m** increases from **6** at $r/R = 0.1$ to **14** at $r/R = 0.6$, and the largest missing data gap spans no more than 30° of azimuth. Hurricanes typically create quasi-continuous precipitation out to $\zeta \approx 150$ km, therefore, the HEVAD method is limited to $R \leq 110$ km where the value of $r/R = 0.45$ is attainable and sufficient for (5)-(10).

Given these restrictions, the procedure for each VAD circle in the LT is as follows: (i) Combine the averages of (9) and (10) with (5) and (6) and insert the results into (7) and (8). (ii) Construct smooth vertical profiles of (5)-(8) by using a Gaussian-weighted filter with an e-folding distance ~0.5 km in the **z** direction. (iii) For each **z** level, combine the smoothed results of (5) and (6) with the averages of (9) and (10) into (1). (iv) Add the smoothed results for (7) and (8) to (2) and (3), respectively, to arrive at the Cartesian components of the earth-relative wind as a function of $\zeta$ and **z**.

## 3. PRELIMINARY TESTS AND CONCLUSIONS

On August 22, 1999, near 23:44 UTC, Hurricane Bret was traveling northwestward toward the Texas

coast at ~3.6 $ms^{-1}$. The WSR-88D radars located at Corpus Christi (KCRP) and Brownsville (KBRO) Texas made near-simultaneous observations of Bret as it passed midway between them over the Gulf of Mexico. KBRO is located at 208-km range and 177° azimuth with respect to KCRP. Fig. 2a shows a PPI-reflectivity image derived from the Archive II data taken from KCRP. KCRP was located between two convective spiral bands north of the eye whereas KBRO was embedded in the stratiform precipitation south of the eye. Figs. 2b and 2c show similarly derived PPI-Doppler velocity images from KCRP and KBRO, respectively. These PPIs were executed with $\theta \approx 0.5^{\circ}$.

Fig. 3a and 3d shows the wind speed contours at 1.5 km altitude, relative to the circulation center at the origin, derived from two different data sources obtained from Peter Dodge of NOAA/AOML/Hurricane Research Division. Fig. 3a was derived from a dual-Doppler synthesis of the KCRP and KBRO volume scan data at this time, and Fig. 3d was derived from a pseudo-dual-Doppler synthesis of radar data collected aboard a NOAA P-3 research aircraft between 23:23 and 23:50 UTC. Note that the 27-minute time resolution of the latter technique tends to smooth the small-scale features, particularly near the strongest winds in the eyewall. Also, the spurious wind values near a line from the N-NW direction to the S-SW direction of Fig. 3a are due to the poor geometry between KCRP and KBRO (Parallel Beams - hereafter referred to as the PB line).

The PCA results from Harasti and List (2001) were used to estimate $\mathbf{R}$, $\zeta_m$, and $\phi_C$ from the data shown in Fig. 2b and 2c. The HEVAD method was applied to the entire Archive II volume scan data for KCRP and KBRO at this time. The smoothed results for the 1.5 km altitude level were computed using an e-folding distance of 1.5 km in the **z** direction. This large e-folding distance was chosen to coincide with that used to derive the results shown in Fig. 3a and 3d. Fig. 3b and 3c show the differences, expressed as percentages, between 3a and the HEVAD wind speeds derived from KBRO and KCRP, respectively. The most important result is that the HEVAD method is able to retrieve both the correct magnitude (67 $ms^{-1}$) and position of the wind maximum in the NW quadrant at $\zeta_m \approx 18$ **km** (note the long-dashed zero-percentage difference contour) for both KBRO and KCRP. The large differences near the PB line are of no concern. Fig. 3e and 3f show the percentage differences between Fig. 3d and the HEVAD wind speeds derived from KBRO and KCRP, respectively. Close inspection of these contours reveal that the absolute biases in the wind field derived from the HEVAD method vary from 0% to 10% *on the side of the hurricane closest to the radar* (south-side for KBRO and north-side for KCRP).

The HEVAD method's estimates of (7) and (8) from KCRP were considerably weaker than those from KBRO, perhaps due to the deformation of the mean flow near the convection. However, the averages of both the KCRP and KBRO results of (7) and (8) agreed well with the calculation of the mean flow across the entire domain of the dual-Doppler winds, as one might expect. The results from this case study seem to suggest that the HEVAD method estimates *the best local fit* of (1) and the mean flow across the VAD circles, and then extrapolates these results with sufficient accuracy out to distances of $\sim (R + \zeta_m)$. Further studies are needed to confirm these very encouraging conclusions.


#### 4. Acknowledgements

The authors are deeply grateful to Mr. Peter Dodge and Dr. Frank Marks Jr. of NOAA/AOML/HRD for allowing us the use of the dual-Doppler wind syntheses of Hurricane Bret. The Natural Sciences and Engineering Research Council of Canada, the Meteorological Service of Canada, the Provincial Government of Ontario and the University of Toronto sponsored the development of the HEVAD method. The UCAR/VSP and the USWRP sponsored these tests of the method.


#### 5. References


Harasti, P.R., and R. List, 2001. See paper P6.12 of these proceedings. Please contact the authors for the remaining references.


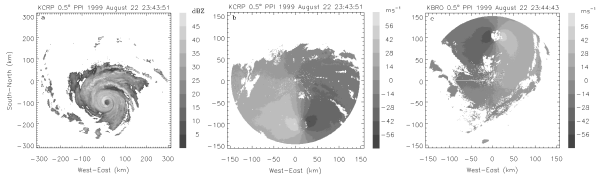

Fig. 2. WSR-88D PPI observations of Hurricane Bret on August 22, 1999, near 23:44 UTC. (a) Reflectivity factor observed at KCRP. (b) and (c) Doppler velocity observed at KCRP and KBRO, respectively.

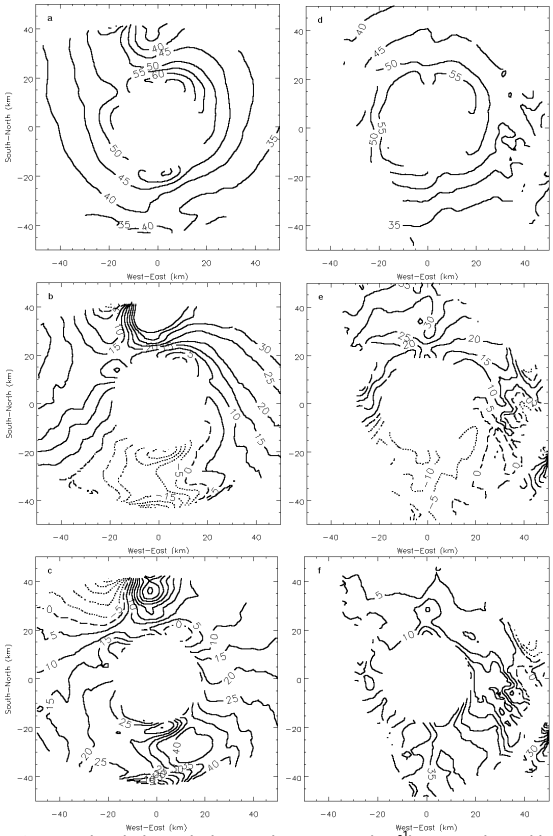

Fig. 3. Earth-relative wind speed contours ($ms^{-1}$) at 1.5-km altitude derived from (a) dual-Doppler synthesis of KCRP and KBRO data, and (d) pseudo-dual Doppler synthesis from the NOAA P-3 aircraft (data courtesy of Peter Dodge, NOAA/AOML/HRD). (b) and (c) show the percentage differences between (a) and the HEVAD wind speeds derived from KBRO and KCRP, respectively. (e) and (f) show the percentage differences between (d) and the HEVAD wind speeds derived from KBRO and KCRP, respectively. The circulation center is at the origin in each plot. See text for more details.